Supporting Information

Self-doped W-WO_x nanocermet multilayer films fabricated by single tungsten target reactive sputtering for selective solar absorption

Wei Wang,[a,b] Huaixing Wen,[b] San Ling,[a] Zhengtong Li,[a] Jingbu Su[a] and Chengbing Wang*[a]

[a]School of Materials Science & Engineering, Shaanxi University of Science & Technology, Xi'an 710021, China

[b]College of Mechanical & Electrical Engineering, Shaanxi University of Science & Technology, Xi'an 710021, China

* Corresponding author. E-mail: wangchengbing@gmail.com

1. Ellipsometry measurements of W-WO_x films

To achieve target solar absorber coatings by single tungsten target reactive sputtering, the evolution of optical properties of W-WO_x films were first investigated. To this end, WO_x monolayers at different oxygen contents were deposited on silicon (100) substrates. Ellipsometry measurements were executed to extract the optical constants of the aforementioned films. The experimentally determined ellipsometer data (amplitude ratio (ψ) and relative phase change (Δ)) were then analyzed by CompleteEASE software. Next, the optical constants were obtained by appropriate theoretical model at precise fittings. **Figure S1** shows the experimental and model fitting data of W-WO_x films at O_2 flow rates of 0, 20, 40, and 100 sccm. The mean squared error (*MSE*) was used to estimate the goodness of fitting between the model and experimental data using the following formulas: [1-3]

$$MSE = \sqrt{\frac{1}{3n-m}\sum_{i=1}^{n}\left[(N_{Ei}-N_{Gi})^2+(C_{Ei}-C_{Gi})^2+(S_{Ei}-S_{Gi})^2\right]}\times 1000 \qquad (1)$$

where n is the number of the determined ellipsometer data and m is the number of fitting parameters.

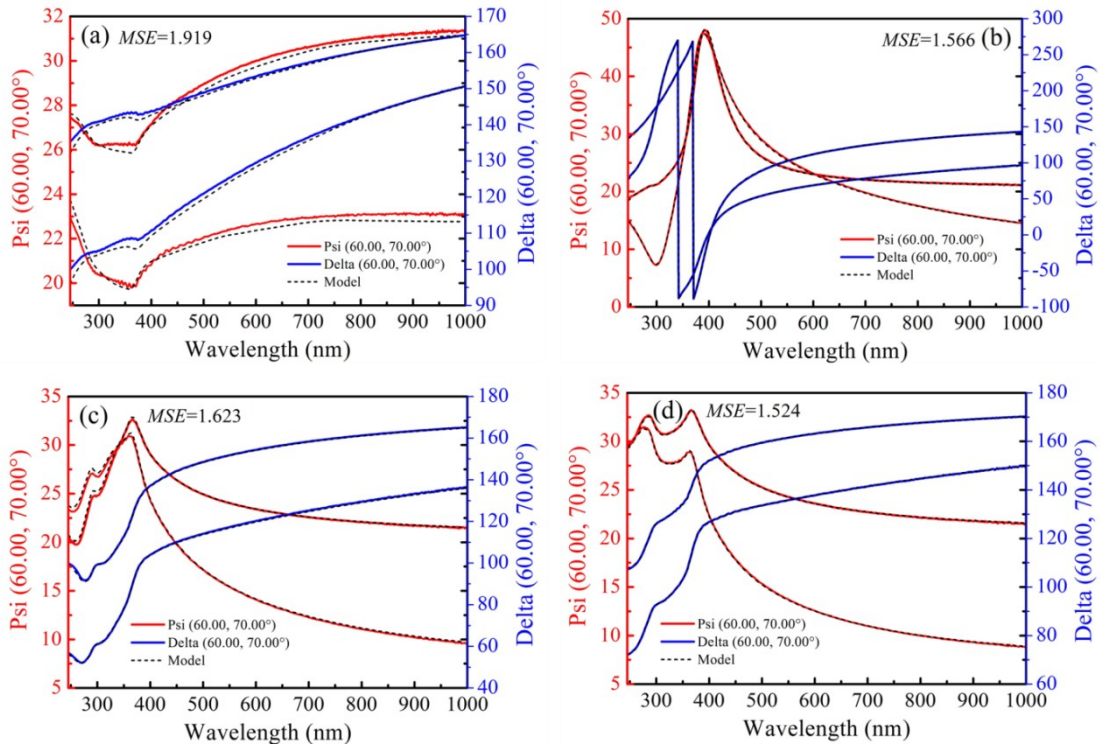

Figure S1. Amplitude ratio (ψ) and relative phase change (Δ) spectra (experimental and model data) of W-WO_x films at O_2 flow rates of (a) 0, (b) 20, (c) 40, and (d) 100 sccm.

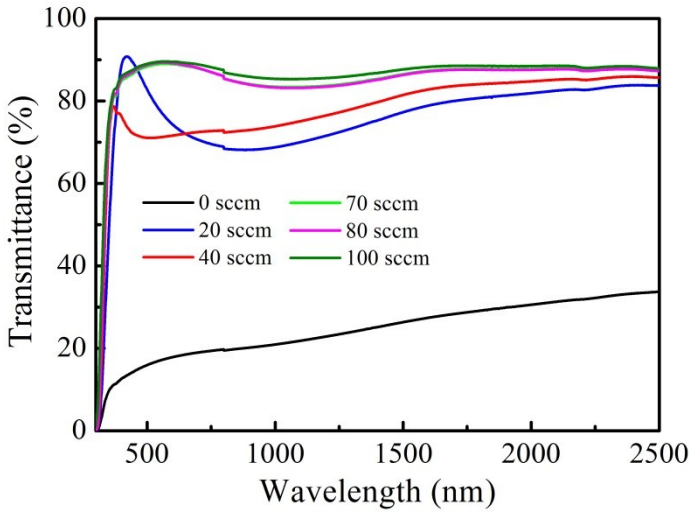

Figure S2. The transmittance spectra of of W-WO_x films at different O_2 flow rates.

Table S1. Optimized parameters of self-doped W-WO_x cermet SSACs.

Layer	Deposition pressure (Pa)	Ar flow rate (sccm)	O_2 flow rate (sccm)	Power (W)	Thickness (min)
Metal W	0.68	60	0	75	42
W-WO_x (HMVF)	0.68	60	20	75	27
W-WO_x (LMVF)	0.73	60	40	100	20
WO_x (AR)	0.88	60	100	100	23

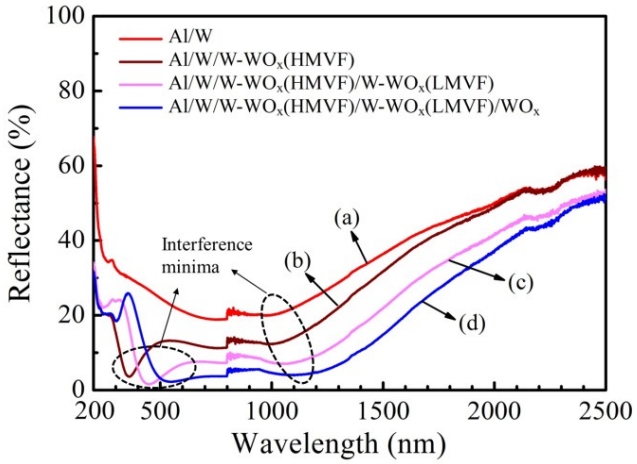

Figure S3. The reflectance spectra of the layer-added W-WO_x SSACs.

Table S2. A summary of the optical absorptivity of reported SSACs.

Solar absorber	Absorptance (α)	Emittance (ε)	Selectivity (α/ε)	Ref.
Mo/AlCrON/AlCrNO/ACrO$_x$	0.921	0.12	7.675	[4]
W/W-Ni-YSZ/W-Ni-YSZ/YSZ/SiO$_2$	0.927	0.059	15.71	[5]
W/W-Ni-Al$_2$O$_3$/W-Ni-Al$_2$O$_3$/Al$_2$O$_3$/SiO$_2$	0.922	0.057	16.17	[6]
Mo/ZrSiN/ZrSiON/SiO2	0.94	0.060	15.67	[12]
W/W-Al$_2$O$_3$/W-Al$_2$O$_3$/Al$_2$O$_3$	0.925	0.070	13.21	[8]
Zr/ZrC-ZrN/ZrO$_x$	0.85	0.10	8.50	[7]
TiC-WC/Al$_2$O$_3$	0.92	0.11	8.36	[9]
TiAlN/TiAlSiN/Si$_3$N$_4$	0.938	0.099	9.47	[14]
W/WTi-Al$_2$O$_3$/WTi-Al$_2$O$_3$/Al$_2$O$_3$	0.93	0.103	9.03	[10]
Mo/TiZrN/TiZrON/SiON	0.95	0.08	11.875	[17]
W/WAlN/WAlON/Al$_2$O$_3$	0.958	0.08	11.98	[11]
Al/NbMoN/NbMoON/SiO$_2$	0.948	0.05	18.96	[13]
MoSi$_2$-Si$_3$N$_4$/MoSi$_2$-Si$_3$N$_4$/Si$_3$N$_4$/Al$_2$O$_3$	0.92	0.13	7.08	[15]
TiAlC/TiAlCN/TiAlSiCN/TiAlSiCO/TiAlSiO	0.961	0.07	13.71	[16]

2. Effect of LMVF and HMVF layers on optical properties

As deposited time of LMVF layer increased (Fig. S4a), the interference peak intensity enhanced. Also, the point of destructive interference changed from one to two and both peak position and cutoff limit shifted to longer wavelengths. On the other hand, as HMVF layer thickness rose (Fig. S4b), the interference peak intensity remained unchanged whereas the position of interference peak and cutoff limit shifted toward longer wavelengths, and lower reflectance observed in the wavelength range of 1000-2500 nm.

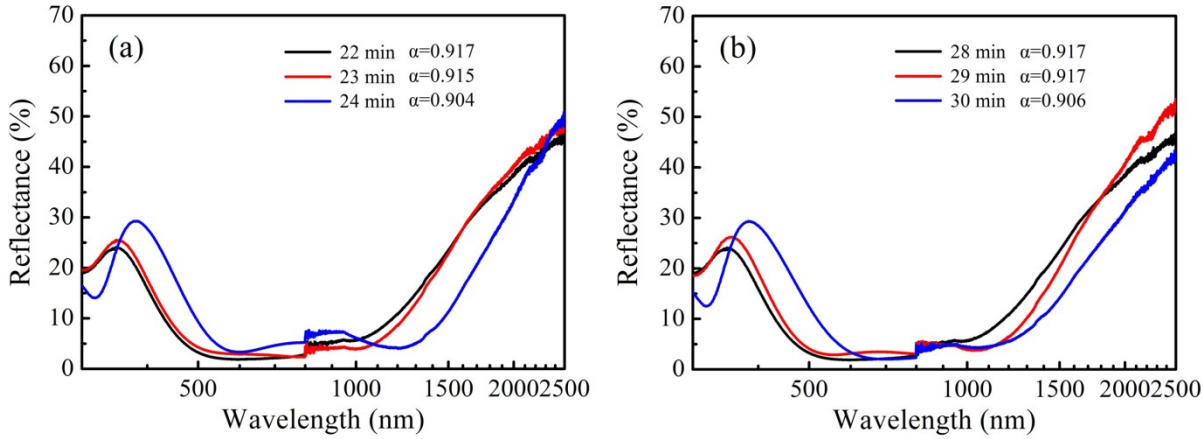

Figure S4. The variation in reflectance spectra of W-WO_x SSACs with different absorbing layers. (a) LMVF layers and (b) HMVF layers.

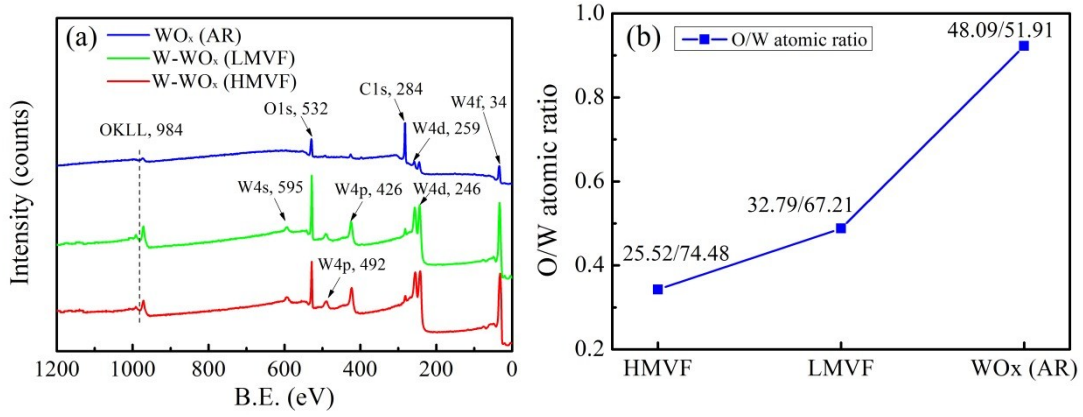

Figure S5. (a) XPS survey spectra and (b) O/W atomic ratio of monolayer in W-WO_x SSACs.

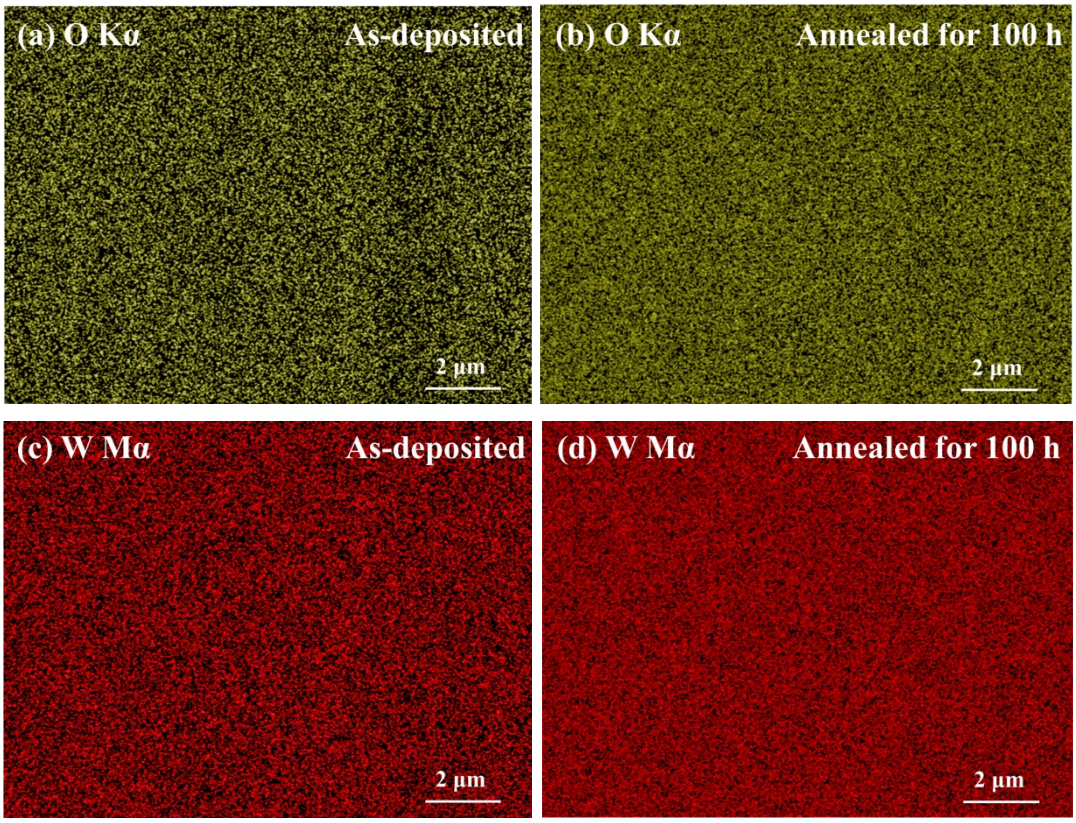

Figure S6. EDS elemental maps of W-WO_x SSACs (a,c) before and (b, d) after annealing for 100 h: (a, b) oxygen and (c, d) tungsten.

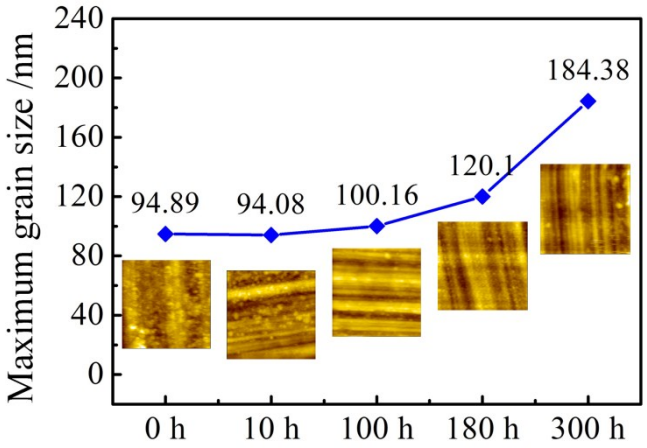

Figure S7. Comparison of maximum grain size of W-WO_x SSACs before and after annealing at 250 °C in air. The insets show the corresponding 2D AFM images.

References

[1] J. P. Meng, X. P. Liu, Z. Q. Fu, K. Zhang, *Sol. Energy*, 2017, **146**, 430-435.

[2] M. Du, L. Hao, J. Mi, F. Lv, X. P. Liu, L, J. Jiang, S. M. Wang, *Sol. Energy Mater. Sol. Cells*, 2011, **95**, 1193-1196.

[3] N. Selvakumar, K. Prajith, A. Biswas, H. C. Barshilia, *Sol. Energy Mater. Sol. Cells*, 2015, **140**, 328-334.

[4] H. D. Liu, T. R. Fu, M. H. Duan, Q. Wan, C. Luo, Y. M. Chen, D. J. Fu, F. Ren, Q. Y. Li, X. D. Cheng, B. Yang, X. J. Hu, *Sol. Energy Mater. Sol. Cells*, 2016, **157**, 108-116.

[5] F. Cao, D. Kraemer, L. Tang, A. P. Livinchuk, J. M. Bao, G. Chen, Z. F. Ren, *Energy Environ*. *Sci.,* 2015, **8**, 3040-3048.

[6] F. Cao, D. Kraemer, T. Sun, Y. C. Lan, G. Chen, Z. F. Ren, *Adv*. *Energy Mater*., 2015, **5**, 1401042.

[7] B. Usmani, A. Dixit, *Sol. Energy*, 2016, **134**, 353-365.

[8] L. Rebouta, A. Sousa, P. Capela, M. Andritschky, P. Santilli, A. Matilainen, K. Pischow, N. P. Barradas, E. Alves, *Sol. Energy Mater. Sol. Cells*, 2015, **137**, 93-100.

[9] X. H. Gao, Z. M. Guo, Q. F. Geng, P. J. Ma, A. Q. Wang, G. Liu, *Sol. Energy Mater. Sol. Cells*, 2017, **164**, 63-69.

[10] X. Y. Wang, J. H. Gao, H. B. Hu, H. L. Zhang, L. Y. Liang, K. Javaid, F. Zhuge, H. T. Cao, L. Wang, *Nano Energy,* 2017, **37**, 232-241.

[11] A. Dan, J. Jyothi, K. Chattopadhyay, H. C. Barshilia, B. Bikramjit, *Sol. Energy Mater. Sol. Cells,* 2016, **157**, 716-726.

[12] Y. P. Ning, W. W. Wang, L. Wang, Y. Sun, P. Song, H. L. Man, Y. L. Zhang, B. B. Dai, J. Y. Zhang, C. Wang, Y. Zhang, S. X. Zhao, E. Tomasella, A. Bousquet, J. Celloer, *Sol. Energy Mater. Sol. Cells,* 2017, **167**, 178-183.

[13] P. Song, Y. X. Wu, L. Wang, Y. Sun, Y. P. Ning, Y. L. Zhang, B. B. Dai, E. Tomasellab, A. Bousquetb, C. Wang, *Sol. Energy Mater. Sol. Cells,* 2017, **171**, 253-257.

[14] J. X. Feng, S. Zhang, Y. L, H. W. Yu, L. M. Kang, X. Y.g Wang, Z. M. Liu, H. C. Ding, Y. Tian, J. Ouyang, *Sol. Energy*, 2015, **111**, 350-356.

[15] A. Rodríguez-Palomo, E. Céspedes, D. Hernández-Pinilla, C. Prieto, *Sol. Energy Mater. Sol. Cells,* 2018, **174**, 50-55.

[16] J. Jyothi, H. Chaliyawala, G. Srinivas, H. S. Nagaraja, H. C. Barshilia, *Sol. Energy Mater. Sol. Cells,* 2015, **140**, 209-216.

[17] Y. Liu, Z. F. Wang, D. Q. Lei, C. Wang, *Sol. Energy Mater. Sol. Cells,* 2014, 1**27**, 143-146.